# CHAOTIC OSCILLATORS USING FREQUENCY-DEPENDENT NEGATIVE RESISTANCE


**BY**

**MR. NATTHORN CHUAYPHAN**


**A THESIS SUBMITTED IN PARTIAL FULFILLMENT OF THE REQUIREMENTS FOR THE DEGREE OF MASTER OF SCIENCE (ENGINEERING AND TECHNOLOGY)**

**SIRINDHORN INTERNATIONAL INSTITUTE OF TECHNOLOGY**

**THAMMASAT UNIVERSITY**

**ACADEMIC YEAR 2021**

THAMMASAT UNIVERSITY
SIRINDHORN INTERNATIONAL INSTITUTE OF TECHNOLOGY

THESIS

BY

MR. NATTHORN CHUAYPHAN

ENTITLED

CHAOTIC OSCILLATORS USING
FREQUENCY-DEPENDENT NEGATIVE RESISTANCE

was approved as partial fulfillment of the requirements for
the degree of Master of Science (Engineering and Technology)

on December 16, 2021

Chairperson _____
(Associate Professor Paiboon Sreearunothai, Ph.D.)

Member and Advisor _____
(Associate Professor Banlue Srisuchinwong, Ph.D.)

Member _____
(Assistant Professor Wimol San-Um, Ph.D.)

Director _____
(Professor Pruettha Nanakorn, D.Eng.)

| | |
|---|---|
| Thesis Title | CHAOTIC OSCILLATORS USING FREQUENCY-DEPENDENT NEGATIVE RESISTANCE |
| Author | Mr. Natthorn Chuayphan |
| Degree | Master of Science (Engineering and Technology) |
| Faculty/University | Sirindhorn International Institute of Technology/ Thammasat University |
| Thesis Advisor | Associate Professor Banlue Srisuchinwong, Ph.D. |
| Academic Years | 2021 |

# ABSTRACT

This thesis presents chaotic oscillators using frequency-dependent negative resistance (FDNR). For the first part, a new algebraically simple five-minimum-term approach to an existing FDNR-based chaotic circuit is presented. An existing piecewise-linear model of a diode is replaced with a new better model using a conventional diode equation. Such a new model results in algebraically simple five minimum terms in three coupled ordinary differential equations (ODEs). Not only are the ODEs reduced from six to five minimum algebraic terms, but also from two nonlinear terms to a single nonlinear term. In particular, a new homoclinic orbit of the circuit is illustrated.

For the second part, a unity-gain approach to a simple FDNR-based chaotic jerk oscillator is proposed. Both unity-gain and FDNR techniques are demonstrated together, for the first time, for a simple chaotic jerk circuit. The proposed chaotic jerk circuit consists of only 7 electronic components, only one of which is an active device. The simplicity results in fewer components of both active and passive devices compared to the existing FDNR-based chaotic circuits. Chaotic attractors, bifurcation diagrams, largest Lyapunov exponents and a Kaplan-Yorke dimension are

demonstrated. The maximized value of the largest Lyapunov exponent is relatively high at 14.62.

**Keywords**: FDNR-based Chaotic Jerk Circuit, Unity-Gain Amplifier, Chaotic Oscillator.

# ACKNOWLEDGEMENTS

First, I offer my sincerest gratitude to my advisor, Associate Professor Banlue Srisuchinwong, Ph.D., for his advice, encouragement, guidance, patience, and support. This thesis would not have been completed without him. I would like to express my appreciation to Assistant Professor Wimol San-Um, Ph.D., for his assistance and suggestions.

Mr. Natthorn Chuayphan

# TABLE OF CONTENTS

# LIST OF TABLES

# LIST OF FIGURES

# CHAPTER 1
# INTRODUCTION

The discovery of the attractor of Lorenz (1963) has attracted great attention to the studies of chaotic circuits and systems. Many applications of chaotic circuits include e.g. chaos-based secure communications (Srisuchinwong & Munmuangsaen, 2011). Some techniques of chaotic circuits have been presented e.g. Srisuchinwong and Amonchailertrat (2013); Srisuchinwong and Munmuangsaen (2012); Srisuchinwong and Nopchinda (2013); Srisuchinwong and Treetanakorn (2014), including a frequency-dependent negative resistance (FDNR) technique. Early examples of FDNR-based chaotic oscillators were reported in e.g. Elwakil and Kennedy (1999, 2000), where a FDNR circuit was introduced as an active linear building block to generate a source of energy, whereas a diode was a passive nonlinear element.

Even though FDNR-based chaotic oscillators have been proposed for more than ten years, publications on this topic have been relatively rare. One of the main reasons for such rare publications is probably that the existing FDNR-based chaotic oscillators do not offer other apparent advantages over other existing approaches.

Recently, a five-term chaotic attractor, e.g. Munmuangsaen and Srisuchinwong (2009), has been reported and the minimum number of algebraic terms in three coupled ordinary differential equations (ODEs) has been clarified to be five terms. Such minimum terms have offered an advantage of simplicity. As the ODEs of the existing FDNR-based chaotic osicllator in Elwakil and Kennedy (2000) have six algebraic terms using the piecewise-linear model for the diode, it is natural to wonder whether that equation may have five minimum terms using a new model by a conventional diode equation.

Although a new algebraically simple five-minimum-term approach to an existing FDNR-based chaotic oscillator has been presented by Chuayphan and Srisuchinwong (2016), as will be the first part of this thesis in chapter 3, the FDNR-based chaotic oscillators have however required two operation amplifiers (op-amps) for FDNR circuit and therefore are not attractive. On the other hand, a unity-gain-based chaotic jerk oscillator has been introduced by Srisuchinwong and Treetanakorn (2014).

Although such a chaotic oscillator has required only a single op-amp, it has however employed not only two active devices, but also a floating diode.

This thesis is separated into two parts. The first part presents a new algebraically simple five-minimum-term approach to an existing FDNR-based chaotic oscillator. The nonlinear element is modeled by replacing an existing piecewise-linear model with a conventional diode equation. The second part presents a unity-gain approach to a simple FDNR-based chaotic jerk oscillator. In particular, the circuit demonstrates the use of not only a FDNR technique, but also only a unity-gain technique for a chaotic jerk oscillator with a grounded diode.

This thesis is organized as follows. Chapter 2 reports background knowledge and related work. Chapter 3 presents the first part of this thesis: a new algebraically simple five-minimum-term approach to an existing FDNR-based chaotic circuit and its new homoclinic orbit, including numerical results. Chapter 4 presents the second part of this thesis: a unity-gain approach to a simple FDNR-based chaotic jerk oscillator, including circuit realization, simulations, and experimental results. Finally, Chapter 5 presents conclusions of the two proposed chaotic oscillators based on FDNR.

# CHAPTER 2
# LITERATURE REVIEWS

## 2.1 Background Knowledge

### 2.1.1 Harmonic Oscillators

One of a simple mechanical system is a harmonic oscillator modeled by a spring-mass-damper system where a mass ($m$) is moving in vertical displacement ($x$) from its equilibrium position by a spring force $-kx$, where $k$ is a spring coefficient. By using the Newton's second law of motion, for the undamped case, the equation of motion is described as

$$m\ddot{x} = -kx \tag{2.1}$$

For the undamped case, the energy is conserved, then the spring keeps going up and down (oscillates) infinitely. In practice, the harmonic oscillator has a form of damping or friction that converts the mechanical energy into heat and eventually the oscillation is suppressed. Such a damping term is referred to by a damper, which adds a damping force of$-Dv = -D\dot{x}$, where $D$ is a damping constant, and $v$ is the velocity. As a result,

$$m\ddot{x} = -D\dot{x} - kx \tag{2.2}$$

The system (2.2) can be rewritten as

$$\ddot{x} = -\alpha\dot{x} - \frac{k}{m}x \tag{2.3}$$

where $\alpha = \frac{D}{m}$ is a damping coefficient. The system (2.3) is called a damped harmonic oscillator.

### 2.1.2 A Feedback Oscillator

In electronics, an oscillator can be implemented through filter network. Such an oscillator can be based on a feedback oscillator or a negative-resistance oscillator.

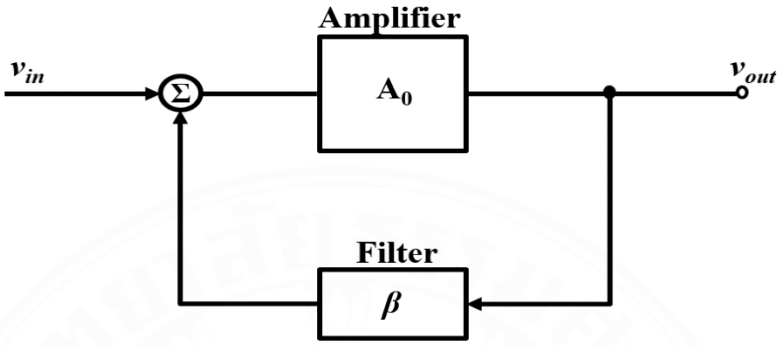


**Figure 2.1** A block diagram of a positive feedback oscillator.

A block diagram of a positive feedback system is shown in Fig. 2.1. The amplifier voltage gain is denoted as $A_0$ (also called an open-loop gain) and the filter transfer function is $\beta$. The closed-loop gain ($A_f$) is expressed as

$$A_f = \frac{A_0}{1-A_0\beta} \tag{2.4}$$

The Barkhausen criterion states that the circuit will sustain steady-state oscillations if: (1) the magnitude of the loop gain is equal to unity, i.e., $|A_0\beta| = 1$, and (2) the phase shift of the loop gain is zero or an integer multiple of $\pm 2\pi$.

### 2.1.3 A Negative-resistance Oscillator

A negative-resistance oscillator employs a resonant circuit and negative resistance as shown in Fig. 2.2. The resonant circuit is typically constructed by an LC-parallel undamped circuit, where the current $i_L$ through the inductor $L$ is in an undamped ODE of the form

$$\ddot{i_L} = -\frac{1}{LC} i_L \tag{2.5}$$

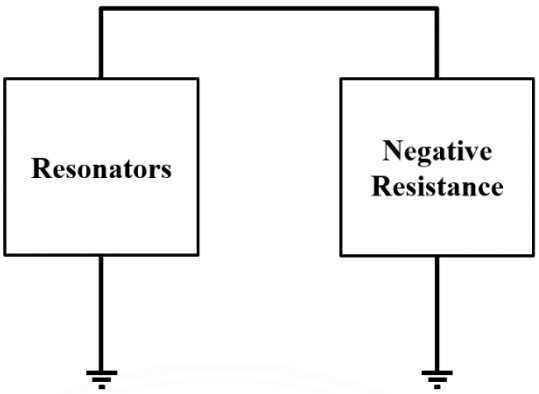


**Figure 2.2** A block diagram of the negative-resistance oscillator.

where the oscillation frequency is $\omega_0 = \frac{1}{\sqrt{LC}}$. In addition, the current $i_L$ in an LC-parallel damped circuit is of the form

$$\ddot{i_L} = -\frac{1}{RC}\dot{i_L} - \frac{1}{LC} i_L \tag{2.6}$$

where $R$ is the parallel resistance.

If the negative resistance of $-R$ is connected in parallel with the resistance $R$, the system (2.6) becomes an undamped ODE and therefore generates oscillations at its resonant frequency $\omega_0$.

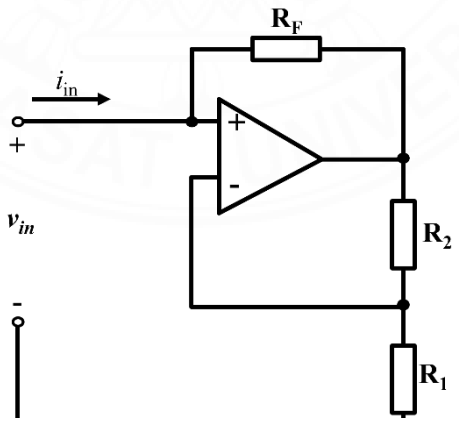


**Figure 2.3** Negative resistance.

### 2.1.4 A Negative Resistance

An example of negative resistance is shown in Fig. 2.3. The equivalent resistance $R_{Th}$ of the circuit is

$$R_{Th} = \frac{v_{in}}{i_{in}} = -\frac{R_L}{A} \tag{2.7}$$

where $A = 1 + \frac{R_2}{R_1}$

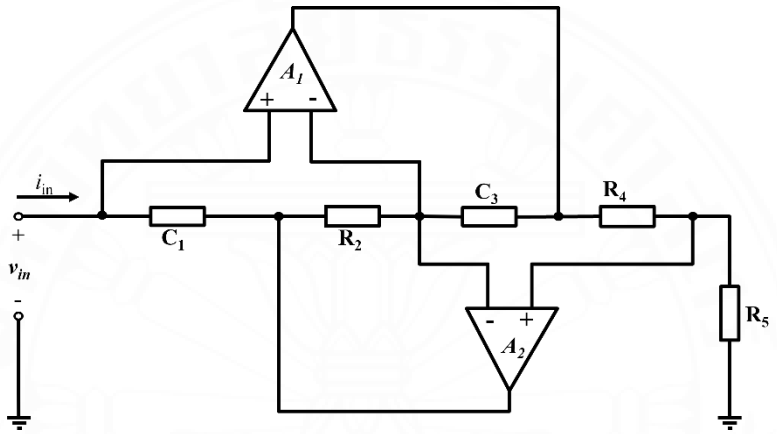


**Figure 2.4** Frequency-dependent negative resistance (FDNR).

### 2.1.5 Frequency Dependent Negative Resistance (FDNR)

Frequency Dependent Negative Resistance (FDNR) is well-known linear building block. An example of FDNR is shown in Fig. 2.4. The equivalent resistance $R_{Th}$ of the circuit is

$$R_{Th} = \frac{1}{Ds^2} = -\frac{1}{D\omega^2} \tag{2.8}$$

where $D$ is

$$D = \frac{C_1 R_2 C_3 R_4}{R_5} \tag{2.9}$$

## 2.2 Chaos Theory

The chaos theory is the study of randomness or unpredictable behavior in systems through mathematical models. Generally, according to Poincare-Bendixon theorem (Hirsch & Smale, 1974), chaos can occur only in at least three-dimensional ODE system. Typically, chaos is determined by three basic properties: very sensitive to initial conditions, topological mixing, and infinite orbits. Hence, Chaos has non-periodic long-term behavior in a deterministic system that exhibits sensitive dependence on initial conditions. Classical examples of chaotic behavior are change of the weather, behavior of the stock markets, biological processes in the living organisms, and fluctuations of the astronomical orbits.

Studies of chaotic circuits have generally been for academic and theoretical reasons. Chaotic circuits were built as physical tools to study nonlinear dynamics described by a set of equations. Mathematicians and theoretical physicists built chaotic circuits to imitate and study dynamics of complex systems. Chaos may offer substantial benefits to many applications, including communications, remote sensing, and cryptography.

## 2.3 Related Work

Sprott (1997) proposed some simple chaotic jerk functions. He showed algebraically simple equations involving ordinary differential equations (ODEs) with quadratic and cubic nonlinearities.

Sprott (2000) proposed simple chaotic systems and circuits. He introduced new chaotic systems with a single third-order ODE with different nonlinearities.

Elwakil and Kennedy (1999) proposed a chaotic oscillator employing frequency dependent negative resistance (FDNR) inspired by Chua's circuit. The structure in Chua's circuit was remained but the Chua's diode was replaced by a parallel connection of FDNR. They showed the relationship between the Rossler's system and the Colpitts-like chaotic circuits.

Elwakil and Kennedy (2000) proposed an improvement of the chaotic oscillator using FDNR by reducing passive components in the structure of Chua's circuit. They presented the design rules to simplify the design process of chaotic oscillators.

Munmuangsaen and Srisuchinwong (2009) proposed a chaotic system with only five terms in three coupled first-order ODE having fewer and simpler terms than those of existing six-term or seven-term chaotic systems.

Munmuangsaen et al. (2011) proposed generalization of the simplest autonomous chaotic system. They discovered some simple chaotic systems of the form $\dddot{x} + \ddot{x} + \dot{x} = f(\dot{x})$.

Sprott (2011) proposed a chaotic jerk circuit. He presented a simple jerk equation which can be implemented by an electronic circuit.

Susan and Jayalalitha (2012) proposed reviews of FDNR. A limitation of using an inductor is that it cannot be appropriated for the micro miniature structure and integrated circuits. Therefore, simulated inductors based on FDNR are used as an alternative.

# CHAPTER 3
# A NEW ALGEBRAICALLY SIMPLE FIVE-MINIMUM-TERM APPROACH TO AN EXISTING FDNR-BASED CHAOTIC CIRCUIT AND ITS NEW HOMOCLINIC ORBIT

## 3.1 Introduction

This chapter introduces a new algebraically simple five-minimum-term approach to an existing FDNR-Based chaotic circuit and its new homoclinic orbit. By replacing an existing piecewise-linear model of a diode with a conventional diode equation, this results in algebraically simple five minimum terms.

## 3.2 An Existing FDNR-based Chaotic Circuit using a Piecewise-Linear Model

An existing FDNR-based chaotic circuit using a piecewise-linear model (Elwakil & Kennedy, 2000) is shown in Fig. 3.1(a), whereas Fig. 3.1 (b) shows the equivalent circuit. The circuit consists of an inductor $L$, a capacitor $C$, a diode $D$ and FDNR denoted as $Z_1$ on the right hand side of node $A$, as shown in Fig. 3.1(b).

### 3.2.1 Frequency-Dependent Negative Resistance (FDNR)

As shown in Fig. 3.1(a), the FDNR $Z_1$ on the right hand side of node $A$ consists of two op-amps $U_1$ and $U_2$, two capacitors $C_1$ and $C_2$, and three resistors $R_1$, $R_2$ and $R$. Let $R_1 = R_2 = R = R_F$, $C_1 = C_2 = C_F$, $K = R/R_F = 1$, impedance $Z_{C1} = 1/(j\omega C_1)$, $Z_{C2} = 1/(j\omega C_2)$, and the complex frequency $s = j\omega$. The FDNR $Z_1$ can be expressed as the form:

$$Z_1 = R\left(\frac{Z_{C1}Z_{C2}}{R_1R_2}\right) = R\left(\frac{-1}{\omega^2 C_1C_2R_1R_2}\right) = \frac{-K}{\omega^2 C_F^2 R_F} = \frac{1}{D_1 s^2} \tag{3.1}$$

where the constant $D_1 = C_F^2 R_F/K$

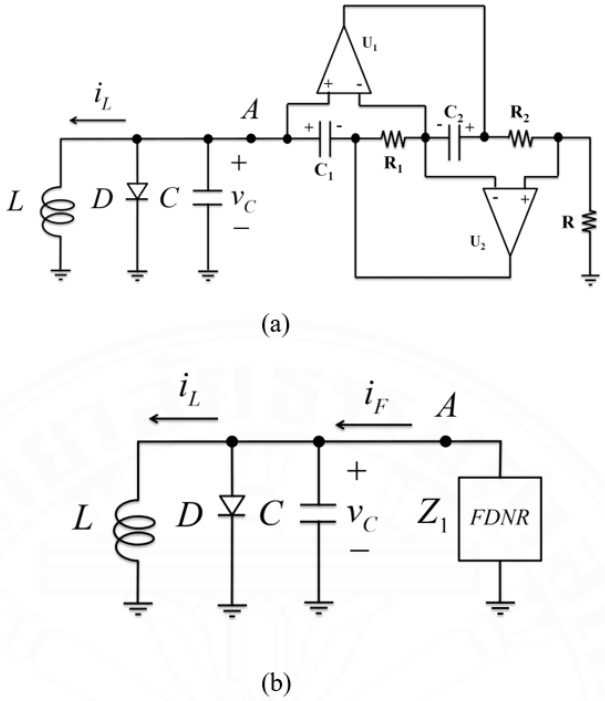


**Figure 3.1** (a) An existing FDNR-based chaotic circuit (Elwakil & Kennedy, 2000), (b) An equivalent circuit where the FDNR is denoted $Z_1$ on the right hand side of node *A*.

### 3.2.2 An Existing Piecewise-Linear Model of the Circuit

Three coupled ODEs of the circuit shown in Fig. 3.1(a) are described by:

$$\begin{cases} D_1\ddot{v_C} = -i_F \\ C\dot{v_C} = -i_F - i_L - I_N \\ L\dot{i_L} = v_C \end{cases} \tag{3.2}$$

where the current $I_N$ through the diode $D$ is approximately described by a piecewise-linear equation of the form

$$I_N = \frac{1}{R_D}\begin{cases} v_C - V_\gamma, v_C \geq V_\gamma \\ 0, v_C < V_\gamma \end{cases} \tag{3.3}$$

and $R_D$ is the diode forward conduction resistance ($\cong 50\ \Omega$), and $V_\gamma$ is the voltage drop ($\cong 0.6\ V$). Let normalized variables $(X, Y, Z)$, normalized constants $(\alpha, \beta)$, normalized time $\tau$, and normalized derivative $(\dot{X}, \dot{Y}, \dot{Z})$, be defined as

$$\begin{bmatrix} \dot{X} & X & \alpha \\ \dot{Y} & Y & \beta \\ \dot{Z} & Z & \tau \end{bmatrix} = \begin{bmatrix} \frac{dX}{d\tau} & \frac{v_C}{V_\gamma} & \frac{R_F}{R_D} \\ \frac{dY}{d\tau} & \frac{R_F i_L}{V_\gamma} & \frac{C_F R_F^2}{L} \\ \frac{dZ}{d\tau} & \frac{dX}{d\tau} & \frac{t}{C_F R_F} \end{bmatrix} \tag{3.4}$$

In this case, $Z = \dot{X}$. Based on (3.4), a normalized dimensionless version of (3.2) using (3.3) is a piecewise-linear dynamical model of the form

$$\begin{bmatrix} \dot{X} \\ \dot{Y} \\ \dot{Z} \end{bmatrix} = \begin{bmatrix} 0 & 0 & 1 \\ \beta & 0 & 0 \\ -aK & -K & -K \end{bmatrix} \begin{bmatrix} X \\ Y \\ Z \end{bmatrix} + \begin{bmatrix} 0 \\ 0 \\ aK \end{bmatrix} \tag{3.5}$$

where $'a'$ is a nonlinear term of the form

$$a = \begin{cases} \alpha, X \geq 1 \\ 0, X < 1 \end{cases} \tag{3.6}$$

It can be noticed that the existing approach on the piecewise-linear model in (3.3) and (3.6) results in six algebraic terms in three coupled ODEs as shown in (3.5). In addition, there are two nonlinear terms of $'a'$ in (3.5). Consequently, (3.5) is not considered to be algebraically simple.

### 3.3 A New Algebraically Simple Five-Minimum-Term Approach using a Diode Equation

The current $I_N$ of the diode $D$ was approximately modeled by a piecewise-linear equation in (3.3). Alternatively, $I_N$ may be better modeled by a conventional diode equation of the form

$$I_N = I_S \left[ \exp\left(\frac{v_C}{nV_T}\right) - 1 \right] \cong I_S \exp\left(\frac{v_C}{nV_T}\right) \tag{3.7}$$

where $V_T$ is the thermal voltage, $n$ is a scaling factor and $I_S$ is the reverse saturation current. Fig. 3.2 shows a comparison of $I_N$ between the existing piecewise-linear model in (3.3), as shown by a dotted line, and the new diode-equation model in (3.7), as shown by a solid line.

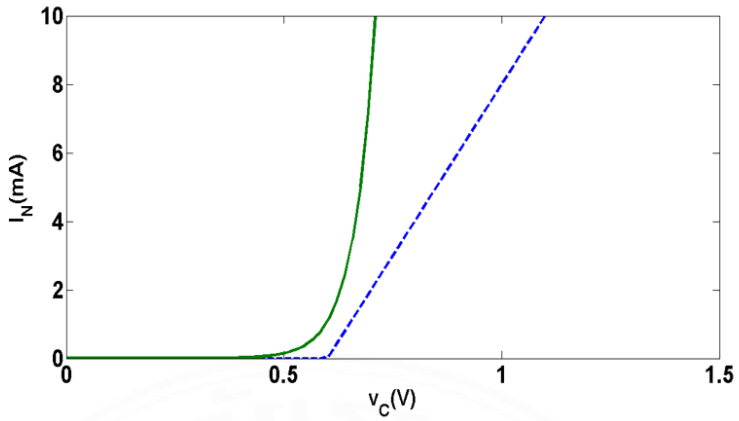


**Figure 3.2** A comparison of $I_N$ between the new (solid line) and the existing (dotted line) models of a diode described in (3.7) and (3.3), respectively.

Let a new normalized constant $A = R_F I_S/(nV_T)$. A new normalized dimensionless version of (3.2) using (3.7) is expressed as a new algebraically simple five-minimum-term approach of the form

$$\begin{bmatrix}\dot{X}\\ \dot{Y}\\ \dot{Z}\end{bmatrix} = \begin{bmatrix}0 & 0 & 1\\ \beta & 0 & 0\\ 0 & -K & -K\end{bmatrix}\begin{bmatrix}X\\ Y\\ Z\end{bmatrix} + \begin{bmatrix}0\\ 0\\ -A\exp(X)\end{bmatrix} \tag{3.8}$$

Unlike the existing six algebraic terms described in (3.5), the new approach in (3.8) is described by only five minimum algebraic terms. In addition, there is only one single nonlinear (exponential) term in (3.8), whereas the existing piecewise-linear approach in (3.5) has two nonlinear terms of $'a'$. Consequently, the new approach in (3.8) is considered to be algebraically simple.

### 3.4 Numerical Results

Trajectories of the new algebraically simple five-minimum-term approach in (3.8) are numerically simulated using the Runge-Kutta integrator with a fixed step side of 0.01. Parameters $C_1$ = $C_2$ = $C_F$ = 10 nF, $C$ = 10 nF, $L$ = 10 mH, $R = R_1 = R_2 = R_F =$ 2 $k\Omega$, $I_S$ = 6.2229 nA, $n$ = 1.9224, $V_T$ = 25.85 mV, and $K$ = 1. Initial conditions of $(X, Y, Z) = (1, 0.5, 0)$.

### 3.4.1 New Better Versions of Chaotic Attractors

For purposes of direct comparisons, chaotic attractors using the existing piecewise-linear approach in (3.5) and (3.6) are numerically depicted in Figs. 3.3(a)-3.3(c), whereas the corresponding chaotic attractors using the new algebraically simple five-minimum-term approach in (3.8) are numerically depicted in Figs. 3.3(d)-3.3(f) on $(X,-Y),(X,Z)$ and $(Y,Z)$ planes, respectively. Note that only Fig 3.3(a) was previously reported in Elwakil & Kennedy (2000) (see Fig. 2 of Elwakil & Kennedy (2000)), whereas Figs. 3.3(b)-3.3(f) are new simulation results presented in this part.

It can be observed from Fig. 3.3 that although chaotic attractors of both approaches are approximately resembled, they are however not exactly the same in some detail. The chaotic attractors in Figs. 3.3(d)-3.3(f) of the new approach show new better versions closely similar to the chaotic attractors obtained from PSpice simulation, whereas the corresponding chaotic attractors in Figs. 3.3(a)-3.3(c) of the existing approach show relatively different versions from those obtained from PSpice simulation. For example, Fig. 3.3(d) is better than Fig. 3.3(a) because Fig. 3.3(d) is much better similar to the chaotic attractor obtained from the PSpice simulation previously reported in Elwakil & Kennedy (2000) (see Fig. 4(b) of Elwakil & Kennedy (2000)). In addition, the reason for such better versions is because the proposed diode equation in (3.7) is a better model for the diode D compared to the existing piecewise-linear model in (3.3), as shown in Fig. 3.2.

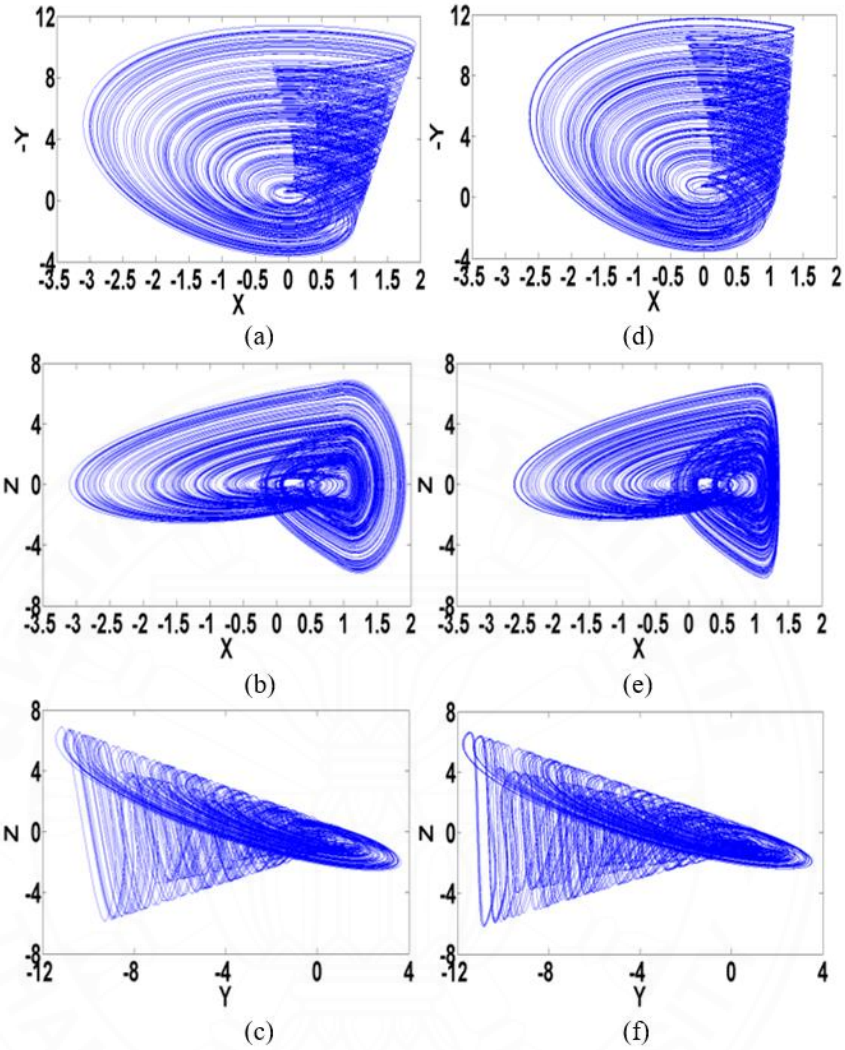


**Figure 3.3** Numerical trajectories on $(X, -Y), (X, Z), (Y, Z)$ planes, respectively,
(a) – (c): Solutions of the existing piecewise-linear approach,
(d) – (f): Solutions of the new algebraically simple five-term approach.

### 3.4.2 New Dynamical results

Fig. 3.4 shows a new numerically bifurcation diagram of the maximum of $X$ $(X - max)$ versus the parameter $K$ from 0 to 4. A period-doubling route to chaos is obvious in Fig. 3.4. Fig. 3.5 illustrates values of a largest Lyapunov exponent $(LLE)$ versus the parameter $K$ from 0 to 4. It can be seen that the chaotic regions shown in Fig. 3.4 are associated with the positive values of the $LLE$ shown in Fig. 3.5.

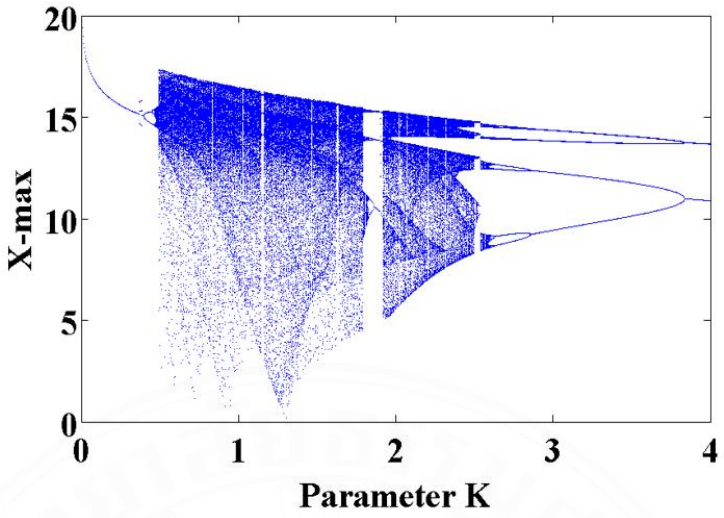


**Figure 3.4** Numerical plots of a bifurcation diagram versus $K$.

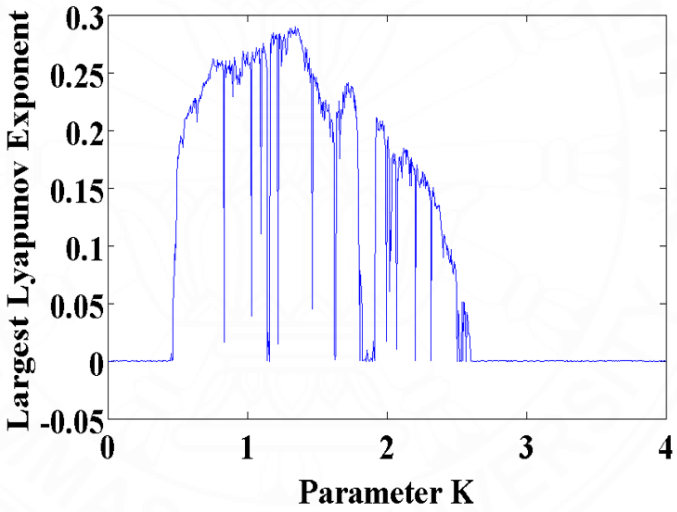


**Figure 3.5** Values of the largest Lyapunov exponent ($LLE$) versus $K$.

### 3.4.3 A New Homoclinic Orbit

The new algebraically simple five-minimum-term approach in (3.8) has an equilibrium point at $(X, Y, Z) = (0, 0, 0)$. The Jacobian matrix at the equilibrium is described as

$$J = \begin{bmatrix} 0 & 0 & 1 \\ B & 0 & 0 \\ -Ae^{X} & -K & -K \end{bmatrix} \tag{3.9}$$

Table 3.1 shows Examples 1 and 2 of eigenvalues $(\lambda_1,\ \lambda_2,\ \lambda_3)$ owning to two different values of $C_F$. Each example has a negative real eigenvalue $(\lambda_1)$ and a complex conjugate pair of eigenvalues $\left(\lambda_{2,3} = \alpha \pm j\beta\right)$ where $\alpha$ is positive. The equilibrium point is therefore a spiral saddle point with an index 2, i.e. the unstable (out-set) manifold has two spatial dimension. As $|\lambda_1| > \alpha$, the Shil'nikov condition (Srisuchinwong & Amonchailertrat, 2013) for a proof of chaos is therefore satisfied. Example 1 represents a general case where the equilibrium point does not locate on the attractor, as shown in Figs. 3.3(d)-3.3(f). On the other hand, Example 2 represents a specific case where the equivalent point intersects the attractor, as shown in Fig. 3.6 by a homoclinic orbit (Srisuchinwong & Amonchailertrat, 2013). Clearly, such an orbit connects the equivalent point to itself on an $(X, Y, Z)$ plane, i.e. the unstable (out-set) manifold intersects the stable (in-set) manifold for a homoclinic connection, and therefore chaos does exist (Srisuchinwong & Amonchailertrat, 2013).

**Table 3.1** Examples 1 and 2 of Eigenvalues

| **Example 1** | **Example 2** |
|---|---|
| $C$ = 10 nF<br>$C_F$ = 10 nF<br>$\lambda_1$ = –1.9999<br>$\lambda_{2,3}$ = 0.5000±$j$1.3229 | $C$ =10 nF<br>$C_F$ = 8.8 nF<br>$\lambda_1$ = –2.0087<br>$\lambda_{2,3}$ = 0.4362±$j$1.2499 |

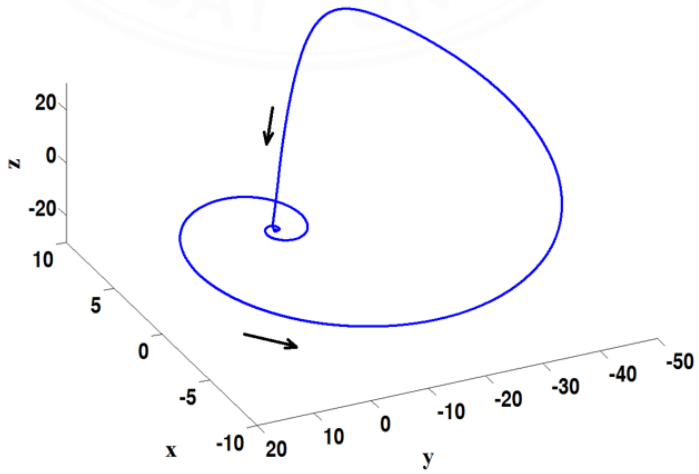


**Figure 3.6** A numerical plot of a homoclinic orbit.

### 3.5 Conclusion

The new algebraically simple five-minimum-term approach to the existing FDNR-based chaotic circuit has been suggested. The existing approximated model of the diode based on the piecewise-linear equation has been replaced with a new better model based on the traditional diode equation. In the three coupled ODEs of the circuit, the existing six algebraic terms have been reduced to the new five minimum algebraic terms, whereas the existing two nonlinear terms have been reduced to only one single nonlinear term. New better versions of chaotic attractors have been compared with those of the existing approach. The bifurcation diagram, the largest Lyapunov exponent, and the homoclinic orbit have been illustrated.

# CHAPTER 4
# A UNITY-GAIN APPROACH TO A SIMPLE FDNR-BASED CHAOTIC JERK OSCILLATOR

## 4.1 Introduction

This chapter introduces a unity-gain approach to a simple FDNR-based chaotic jerk oscillator.

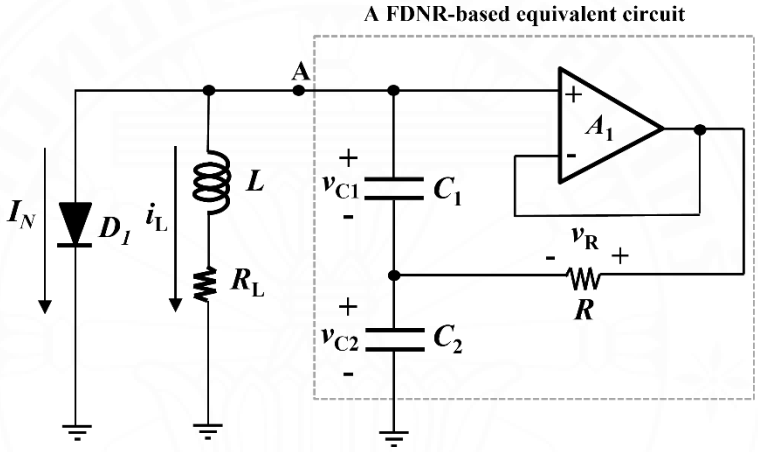


**Figure 4.1** A unity-gain approach to a simple FDNR-based chaotic jerk oscillator.

## 4.2 Circuit realisation

Fig. 4.1 shows the proposed chaotic jerk oscillator using unity-gain-based FDNR. The circuit consists of two parts separated by node $A$. The first part, as shown on the left side of node $A$, consists of a grounded diode $D_1$ for the necessary nonlinearity, an inductor $L$, and a resistor $R_L$ including the internal resistance of $L$. The second part (Pookaiyaudom, 2006; Senani, 1985), as shown on the right side of node $A$, consists of an op-amp $A_1$ of a unity-gain amplifier, capacitors $C_1$ and $C_2$, and a resistor $R$. Fig. 4.1 is therefore described by a set of three coupled first-order ordinary differential equations (ODEs) of the form:

$$\begin{cases} \dot{v_{C1}} = -\frac{i_L}{C_1} - \frac{I_N}{C_1} \\ \dot{v_{C2}} = -\frac{v_{C1}}{RC_2} - \frac{i_L}{C_2} - \frac{I_N}{C_2} \\ \dot{i_L} = \frac{v_{C1}}{L} + \frac{v_{C2}}{L} - \frac{i_L R_L}{L} \end{cases} \tag{4.1}$$

where the diode current $I_N$ of $D_1$ is of the form

$$I_N = I_S\left[\exp\left(\frac{v_{C1}+v_{C2}}{nV_T}\right) - 1\right] \tag{4.2}$$

and $I_S$ is the saturation current of $D_1$, $V_T$ is the thermal voltage, and $n$ is the scaling factor.

Let (4.3) define constants $A, B, E, F$, and $G$, dimensionless normalized variables $X, Y$, and $Z$, and dimensionless normalized time $\tau$, where $t$ is time, time constants $\tau_L = L/R_L$ , $\tau_1 = R_L C_1$, $\tau_2 = R_L C_2$, $\tau_3 = RC_2$, resistor $R_L = R_1 + R_2$, $R_1$ is parasitic resistance of $L$, and $R_2$ is a resistor.

$$\begin{bmatrix} \dot{X} & X & A & F \\ \dot{Y} & Y & B & G \\ \dot{Z} & Z & E & \tau \end{bmatrix} = \begin{bmatrix} \frac{dX}{d\tau} & \frac{v_{C1}}{nV_T} & \frac{\tau_L}{\tau_1} & \frac{\tau_L I_S}{nV_T C_1} \\ \frac{dY}{d\tau} & \frac{v_2}{nV_T} & \frac{\tau_L}{\tau_3} & \frac{\tau_L I_S}{nV_T C_2} \\ \frac{dZ}{d\tau} & \frac{i_L R_L}{nV_T} & \frac{\tau_L}{\tau_2} & \frac{t}{\tau_L} \end{bmatrix} \tag{4.3}$$

The set of ODEs in (4.1) can be normalized and represented by

$$\begin{bmatrix} \dot{X} \\ \dot{Y} \\ \dot{Z} \end{bmatrix} = \begin{bmatrix} 0 & 0 & -A \\ B & 0 & -E \\ 1 & 1 & -1 \end{bmatrix} \begin{bmatrix} X \\ Y \\ Z \end{bmatrix} + \begin{bmatrix} -F\exp(X+Y) \\ -G\exp(X+Y) \\ 0 \end{bmatrix} \tag{4.4}$$

In addition, (4.4) can be transformed to a jerk equation of the form

$$\dddot{Z} = -a_0\ddot{Z} - a_1\dot{Z} - a_2 Z - a_3\exp\left(Z + \dot{Z}\right) \tag{4.5}$$

where

$$\begin{aligned} a_0 &= 1 + (F+G)\exp\left(Z+\dot{Z}\right) \\ a_1 &= (A+E) + (F+G)\exp\left(Z+\dot{Z}\right) \\ a_2 &= AB \\ a_3 &= BF \end{aligned} \tag{4.6}$$

### 4.3 An equivalent circuit of the proposed circuit

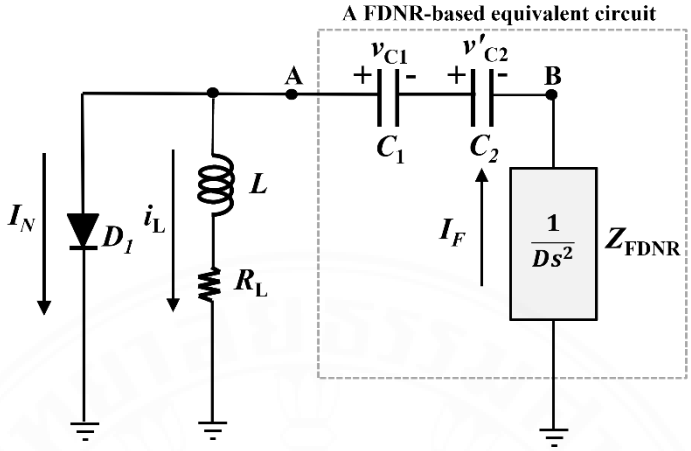


**Figure 4.2** An equivalent circuit of Fig. 1 based on an FDNR.

Fig. 4.2 shows an equivalent circuit of Fig. 4.1. The first part, as shown on the left side of node $A$, remains the same as that of Fig. 4.1, whereas the second part, as shown on the right side node $A$, is modelled by a FDNR-based equivalent circuit, of which the Thevenin equivalent impedance is a series circuit (Pookaiyaudom, 2006) consisting of capacitors $C_1$ and $C_2$, and FDNR of the form $Z_{FDNR} = 1/(Ds^2)$ where $D = C_1C_2R$. Fig. 4.2 is described by ODEs of the form:

$$\begin{cases} \dot{v_{C1}} = -\frac{i_F}{C_1} \\ \dot{v'_{C2}} = -\frac{i_F}{C_2} \\ \dot{i_L} = -\frac{i_L R_L}{L} + \frac{v_{C1}}{L} + \frac{v'_{C2}}{L} - \frac{v_B}{L} \end{cases} \tag{4.7}$$

where $v_A$ and $v_B$ are voltages at nodes $A$ and $B$, respectively, with respective to ground, and

$$\begin{aligned} I_F &= -D\ddot{v_B} = i_L + I_N \\ v_B &= v_A - v_{C1} - v'_{C2} \\ v_{C2} &= v'_{C2} + v_B \\ I_N &= I_S\left[\exp\left(\frac{i_L R_L + L\dot{i_L}}{nV_T}\right) - 1\right] \end{aligned} \tag{4.8}$$

with reference to Fig. 4.2, let (4.9) define constants $a$, $b$, $d$, $f$, and $g$, dimensionless normalized variables $Z, \dot{Z}, \ddot{Z}$ and $\dddot{Z}$.

$$\begin{bmatrix} \dot{Z} & Z & d \\ \ddot{Z} & a & f \\ \dddot{Z} & b & g \end{bmatrix} = \begin{bmatrix} \frac{dZ}{d\tau} & \frac{i_L R_L}{nV_T} & \frac{\tau_L I_S}{nV_T C_1} \\ \frac{d^2Z}{d\tau^2} & \frac{{\tau_L}^3}{LC_1C_2R} & \frac{\tau_L I_S}{nV_T C_2} \\ \frac{d^3Z}{d\tau^3} & \frac{{\tau_L}^2}{LC_1} + \frac{{\tau_L}^2}{LC_2} & \frac{{\tau_L}^2 I_S}{nV_T C_1 C_2 R} \end{bmatrix} \tag{4.9}$$

The set of ODEs in (4.7) can be normalized and described by a jerk equation of the form

$$\dddot{z} = -a_4\ddot{z} - a_5\dot{z} - a_6 z - a_7 \exp\left(Z + \dot{Z}\right) \tag{4.10}$$

where

$$\begin{aligned} a_4 &= 1 + (d+f)\exp\left(Z + \dot{Z}\right) \\ a_5 &= b + (d+f)\exp\left(Z + \dot{Z}\right) \\ a_6 &= a \\ a_7 &= g \end{aligned} \tag{4.11}$$

It is found that the jerk equation in (4.5) of Fig. 4.1 is equal to the jerk equation in (4.10) of Fig. 4.2, as parameters (4.6) of Fig. 4.1 are equal to parameters (4.11) of Fig. 4.2, respectively, as follows:

$$\begin{aligned} (F+G) = (d+f) &= \left(\frac{I_S L}{nV_T C_1 R_L}\right) + \left(\frac{I_S L}{nV_T C_2 R_L}\right) = 3.306 \times 10^{-4} \\ (A+E) = b &= \left(\frac{L}{C_1 R_L^2}\right) + \left(\frac{L}{C_2 R_L^2}\right) = 189.1253 \\ AB = a &= \left(\frac{L^2}{RC_1C_2{R_L}^3}\right) = 4.4710 \times 10^5 \\ BF = g &= \left(\frac{I_S L^2}{RC_1C_2R_L^2 nV_T}\right) = 0.7810 \end{aligned} \tag{4.12}$$

Such consistency verifies that the proposed unity-gain chaotic jerk circuit as shown in Fig. 4.1 is indeed modelled by the equivalent circuit based on the FDNR as shown in Fig. 4.2. In addition, both jerk equations in (4.5) of Fig. 4.1 and that in (4.10) of Fig. 4.2 correspond to the same jerk of the form

$$\begin{aligned}\dddot{i}_L = &-\left[\frac{R_L}{L}+\left(\frac{I_S}{nV_TC_1}+\frac{I_S}{nV_TC_2}\right)\exp(i_LR_L+L\dot{i}_L)/nV_T\right]\ddot{i}_L\\ &-\left[\frac{1}{LC_1}+\frac{1}{LC_2}+\left(\frac{R_LI_S}{nV_TLC_1}+\frac{R_LI_S}{nV_TLC_2}\right)\exp(i_LR_L+L\dot{i}_L)/nV_T\right]\dot{i}_L\\ &-\frac{i_L}{C_1C_2RL}-\left(\frac{I_S}{C_1C_2RL}\right)[\exp(R_Li_L+L\dot{i}_L)/nV_T]\end{aligned} \tag{4.13}$$

It can be observed that the proposed chaotic jerk oscillator enables a nonlinear damping coefficient, as shown in parameter $a_0$ of (4.6) of Fig. 4.1, in parameter $a_4$ of (4.11) of Fig. 4.2, and in (4.13) of both Figs. 4.1 and 4.2.

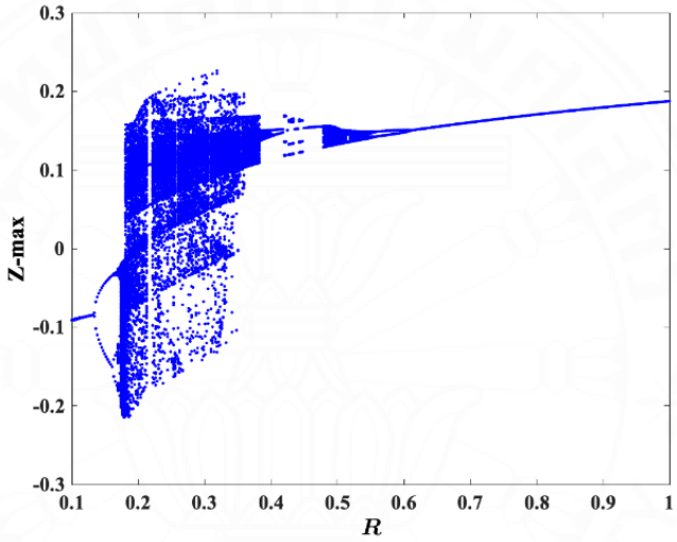


**Figure 4.3** A bifurcation diagram of $Z-max$ against $R$.

### 4.4 Simulations and experiments

Numerical simulations of jerk trajectories in (4.5) use the Runge-Kutta integrator, an adaptive step size (time step ≤ 0.001), and values of $R$ = 0.3 Ω, $R_L = R_1 + R_2 = 15\Omega$, $R_1 = 2.7\Omega$, $R_2 = 12.3\Omega$, $C_1 = C_2 = C$= 47 nF, $L$ = 1 mH, $I_S$ = 5.84 nA, $V_T$ = 25.85 mV, and $n$ = 1.94. The op-amp $A_1$ is TL082 and the diode $D_1$ is 1N4148. Real experiments of jerk trajectories in (4.5) use measured values of $R$ = 5.2Ω, $R_L = R_1 + R_2 = 11.15\Omega$, $R_1 = 2.7\Omega$, $R_2 = 8.45\Omega$, $C_1 = C_2 = C$ = 47 nF, $L$ = 1 mH. Although initial conditions are not critical, they are chosen at $(Z_0, \dot{Z}_0, \ddot{Z}_0) = (0.001, 0, 0)$ close to the attractor to reduce initial transients.

Fig.4.3 shows numerical plots of a bifurcation diagram of the peak of $Z$, denoted as $Z-max$, against the resistance $R$. Figs. 4.4 and 4.5 depict the corresponding largest

Lyapunov exponent $(LLE)$ and the Kaplan-Yorke dimension $(D_{KY})$ against the resistance $R$, respectively. The maximized value of the $LLE$ is 14.62 at $R = 0.1923\Omega$. The maximized value of the $D_{KY}$ is 2.259 at $R = 0.1855\Omega$. Figs. 4.6(a) to 4.6(c) illustrate numerical trajectories of attractors of (4.5) for $R = (13, 0.4, 0.3)\Omega$, respectively, on a $[Z, f(\ddot{Z}, \dot{Z}, Z)]$ plane, where $f(\ddot{Z}, \dot{Z}, Z) = Y$ of the form

$$Y = \frac{-\ddot{Z} - (1-B)\dot{Z} - (A-B+E)Z - (F+G)\exp(z+\dot{z})}{B} \tag{4.14}$$

Figs. 4.6(d) to 4.6(f) depict oscilloscope traces of Fig. 4.1 for $R = (13.77, 8.4, 5.2)\Omega$, respectively, on an $[i_L R_2, v_{C2}]$ plane, where $i_L R_2$ corresponds to a scaled $Z$, and $v_{C2}$ corresponds to a scaled $Y$. In Fig. 4.6, the numerical results are in good agreements with the experimental results.

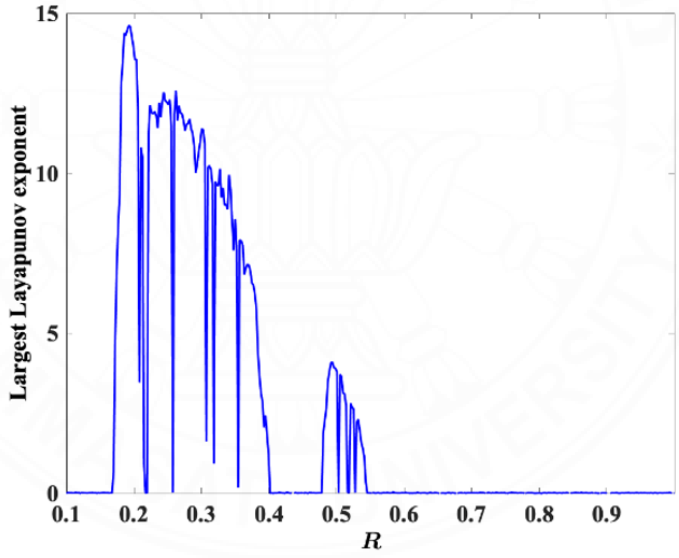


**Figure 4.4** The largest Lyapunov exponent $(LLE)$ against $R$.

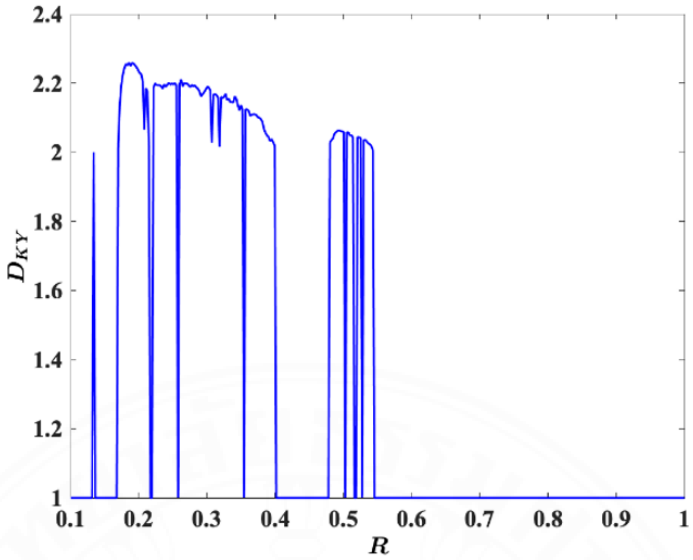


**Figure 4.5** The Kaplan-Yorke Dimension $(D_{KY})$ against $R$.

### 4.5 Comparisons with existing FDNR-based chaotic circuits

Table 1 shows comparisons of the proposed unity-gain FDNR-based chaotic jerk oscillator with existing FDNR-based chaotic oscillators (Chuayphan & Srisuchinwong, 2016; Elwakil & Kennedy, 1999, 2000). Table 1 shows that the existing FDNR-based chaotic oscillators are not chaotic jerk oscillators, but require many electronic components of 10 to 12, two of which are active devices.

This Chapter not only demonstrates, for the first time, a unity-gain approach to a simple FDNR-based chaotic jerk oscillator, but also requires fewer components, i.e., only 7 components, only one of which is an active device. In addition, the maximized value of the $LLE$ is 14.62, which is larger than that of the existing FDNR-based chaotic circuits.

### 4.6 Conclusion

The unity-gain approach to a simple FDNR-based chaotic jerk oscillator has been presented for the first time. The circuit requires only a single active component and only 7 components in total. This results in fewer components in both active and passive devices compared to existing FDNR-based chaotic circuits. The numerical and experimental results are consistent. The bifurcation diagram, the $LLE$ and the Kaplan-

Yorke dimension have been illustrated. The maximized value of the *LLE* at 14.62 is relatively high.

**Table 4.1** Comparisons with existing FDNR-based chaotic circuits.

| No. | Terms of Comparison | References | | | |
|---|---|---|---|---|---|
| | | Elwakil & Kennedy (1999) | Elwakil & Kennedy (2000) | Chuayphan & Srisuchinwong (2016) | This work |
| 1. | FDNR technique | ✓ | ✓ | ✓ | ✓ |
| 2. | Unity-gain technique | × | × | × | ✓ |
| 3. | Jerk equation | × | × | × | ✓ |
| 4. | The maximized *LLE* | × | × | 0.28 | 14.62 |
| 5. | The maximized $D_{KY}$ | × | × | × | 2.259 |
| 6. | No. of active devices | 2 | 2 | 2 | 1 |
| 7. | No. of passive components | 10 | 8 | 8 | 6 |
| 8. | Total components | 12 | 10 | 10 | 7 |

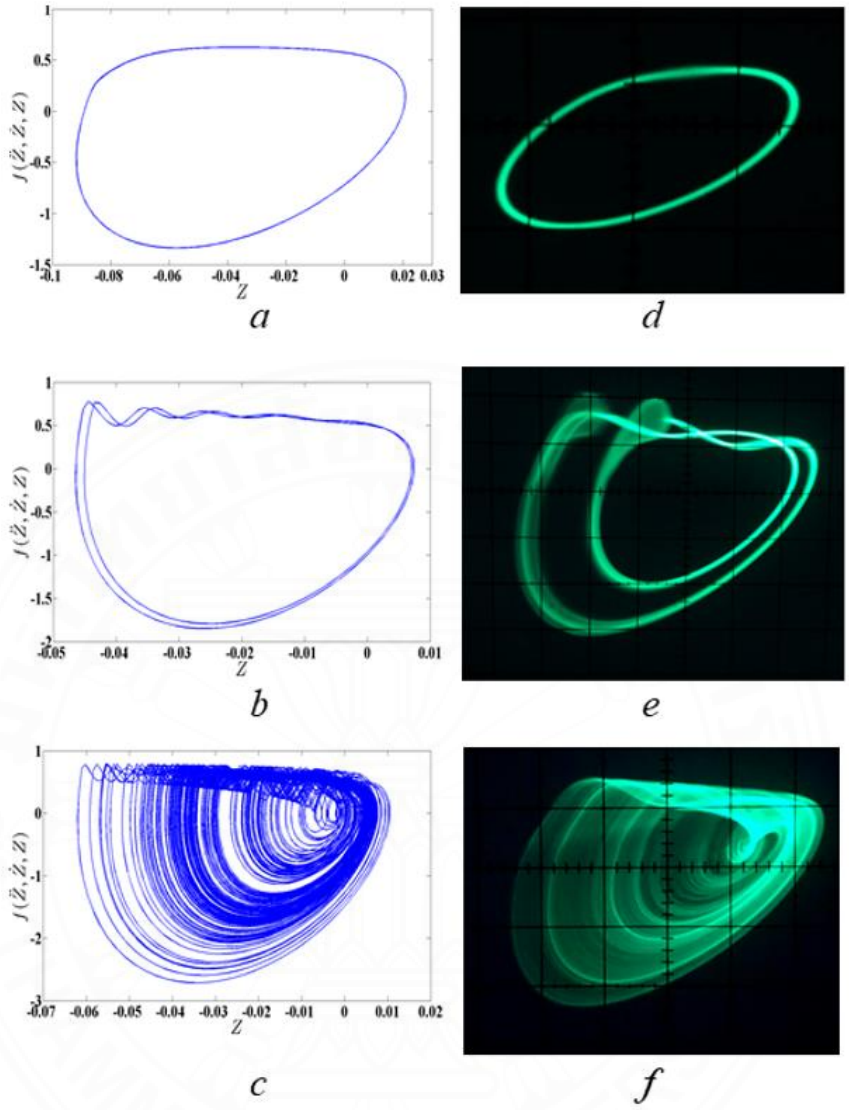


**Figure 4.6** (a)-(c): Numerical trajectories on a $[Z, f(\ddot{Z},\ \dot{Z}, Z)]$ plane.
(d)-(f): Oscilloscope traces on an $[i_L R_2, v_{C2}]$ plane.

# CHAPTER 5
# CONCLUSION

The thesis consists of two main parts. In the first part of this thesis, as shown in chapter 3, the new algebraically simple five-minimum-term approach to an existing FDNR based chaotic circuit has been proposed. By substitute the existing nonlinear term with the Shockley diode equation, the existing six algebraic terms in the three coupled ODEs of the circuit have been reduced to the new five minimum algebraic terms, whereas the two nonlinear terms have been reduced to only a single nonlinear term. The better versions of chaotic attractors, the bifurcation diagram and the largest Lyapunov exponent are depicted. In particular, a new homoclinic orbit of the proposed circuit of the first part is illustrated.

In the second part of this thesis, as shown in chapter 4, the unity-gain approach to a simple FDNR-based chaotic jerk oscillator has been presented. The unity-gain technique and the FDNR-based technique are demonstrates together for a simple chaotic jerk circuit together for the first time. The proposed circuit requires only a single active component and only 7 components in total compared with the existing FDNR-based chaotic circuits. The configuration of FDNR in this part has been based on a unity-gain amplifier. The numerical results are good agreements with the experimental results. The maximized value of the largest Lyapunov exponent is relatively high at 14.62.

# REFERENCES

Chuayphan, N. & Srisuchinwong, B. (2016). A new algebraically simple five-minimum-term approach to an existing FDNR-based chaotic circuit and its new homoclinic orbit. *International Symposium on Fundamental Electrical Engineering*, (pp. 1 – 4).

Elwakil, A. S. & Kennedy, M. P. (1999). Chaotic oscillator configuration using a frequency dependent negative resistor. *Journal of Circuits, Systems and Computers*, *9*, 229 – 242.

Elwakil, A. S. & Kennedy, M. P. (2000). Chaotic oscillator configuration using a frequency dependent negative resistor. *International Journal of Circuit Theory and Applications*, *28*, 69 – 76.

Hirsch, M. & Smale, S. (1974). *Differential Equations, Dynamical Systems and Linear Algebra.* San Diego: Academic Press.

Lorenz, E. N. (1963). Deterministic nonperiodic flow. *Journal of the Atmospheric Sciences*, *20*, 130 – 141.

Munmuangsaen, B. & Srisuchinwong, B. (2009). A new five-term simple chaotic attractor. *Physics Letters A*, *373*, 4038 – 4043.

Munmuangsaen, B., Srisuchinwong, B., & Sprott, J. C. (2011). Generalization of the simplest autonomous chaotic system. *Physics Letters A*, *375*(12), 1445 – 1450.

Pookaiyaudom, S. (2006). *Negative feedback circuits and oscillators.* Bangkok: Mahanakorn University of Technology.

Senani, R. (1985). New rc-active oscillator configuration employing unity-gain amplifier. *Electronics Letters, 21*(20), 889–890.

Sprott, J. C. (1997). Some simple chaotic jerk functions. *American Journal of Physics, 65*(6), 537 – 543.

Sprott, J. C. (2000). Simple chaotic systems and circuits. *American Journal of Physics, 68*(8), 758 – 763.

Sprott, J. C. (2011). A new chaotic jerk circuit. *Circuits and Systems II: Express Briefs, IEEE Transactions*, *58*(4), 240 – 243.

Srisuchinwong, B. & Amonchailertrat, N. (2013). Realization of a lambert w-function for a chaotic circuit. *Journal of Circuits, Systems and Computers, 22*(8), 1 – 12.

Srisuchinwong, B. & Munmuangsaen, B. (2011). Secure communication systems based upon two-fold masking of different chaotic attractors, including modified chaotic attractors, using static-dynamic secret keys. Retrieved from http://www.wipo.int/patentscope/search/en/WO2011105972. WO2011105972.

Srisuchinwong, B. & Munmuangsaen, B. (2012). Four current-tunable chaotic oscillators in set of two diode-reversible pairs. *Electronics Letters, 48*(17), 1051 – 1053.

Srisuchinwong, B. & Nopchinda, D. (2013). Current-tunable chaotic jerk oscillator. *Electronics Letters, 49*(9), 587 – 589.

Srisuchinwong, B. & Treetanakorn, R. (2014). Current-tunable chaotic jerk circuit based on only one unity-gain amplifier. *Electronics Letters, 50*(24), 1815 – 1817.

Susan, D. & Jayalalitha, S. (2012). Frequency dependent negative resistance-a review. *Research Journal of Applied Sciences, Engineering and Technology, 4*(17), 2988 – 2994

# BIOGRAPHY

| | |
|---|---|
| Name | Mr. Natthorn Chuayphan |
| Education | 2014: Bachelor of Engineering (Computer Engineering)<br>Thai-Nichi Institute of Technology |

Publications

Chuayphan, N. & Srisuchinwong, B. (2016). A new algebraically simple five-minimum-term approach to an existing FDNR-based chaotic circuit and its new homoclinic orbit. *Proceedings of International Symposium on Fundamental Electrical Engineering* (pp.1-4).

Chuayphan, N. & Srisuchinwong, B. (2021). *A unity-gain approach to a simple FDNR-based chaotic jerk oscillator.* (Submitted to Electronics Letters)

San-Um, W. & Chuayphan, N. (2014). A Lossless physical-layer encryption scheme in medical Picture Archiving and Communication Systems using highly-robust chaotic signals. *Proceedings of the 7th Biomedical Engineering International Conference* (pp. 1-5).